Modeling generalized stacking fault in Au using tight-binding potential combined with a simulated annealing method

Jun Cai and Jian-Sheng Wang

Abstract—

Tight-binding potential combined with a simulated annealing method is used to study the generalized stacking fault structure and energy of gold. The potential is chosen to fit band structures and total energies from a set of first-principles calculations (Phys. Rev. B54, 4519(1996)). It is found that the relaxed stacking fault energy (SFE) and anti-SFE are equal to 46 and 102 mJ/m^2, respectively, and in good agreement with the first principles calculations and experiment. In addition, the potential predicts that the c/a of hcp-like stacking fault structure in Au is slightly smaller than the ideal one.

Keywords— **Generalized stacking fault, Tight-binding potential, Au.**

I. Introduction

THE atomic-scale structure of generalized stacking fault (GFS), just like grain boundaries, is considerable interest to materials research. This is due to the fact that the stacking fault impacts strongly the mechanical properties of materials. For example, the stability of stacking faults on the slip planes of a crystal is intimately connected to the mobility of dislocations on these planes[1]. Likewise, in low stacking fault energy metals many interfaces may relax by emitting stacking faults so that extend the structural perturbation of these interfaces over several planes normal to the interfaces[2]. Moreover, Martensitic transformation in shape-memory alloys[3] is directly related to stacking fault. Certainly, it is also well known that twining stress increases with increasing stacking fault energy for the most of fcc metals[4]. etc. Based on these reasons, the stacking faults of metals have been studied both experimentally and theoretically, even for fcc mono-metals (see, for examples, [1], [2], [4], [5], [6], [7], [8]).

On the other hand, a theoretical study for GSF may be used to test the reliability of a theoretical model, especially for developing an atom potential model. In the recent works Zimmerman et al used embedded-atom potentials to calculate GFS energies of Al, Ni, and Cu, and found that in the most cases the embedded-atom potentials underestimated SFE and anti-SFE[5]. At the same time Mehl et al used a tight-binding (TB) potential to study the SFE and anti-SFE of fcc metals Al, Cu, Rh, Pd, Ag, Ir, Au, and Pb. They compared their results with full potential linear-muffin orbital and embedded-atom potential calculations, as well as experiment, and found good agreement. This is impressive, since their tight-binding potential only fits to first-principles full-potential linearized augmented plane-wave equations of state and band structures for cubic systems. Comparable accuracy with embedded-atom potentials can be achieved only by fitting to the stacking fault energy[1]. But, regretly, in their calculations, the atom relaxation was not considered, expect for the the case of anti-SFE of Au and Ir. Also they did not present any information about relaxed GSF structures. In fact, to our knowledges, a detail picture about GFS structure considering atom-scale relaxation is lack. It is also surprising that in the works of Zimmerman et al, there are not any information about the relaxed GFS structures, too, although an atom relaxation is included. Thus, in this work, as an example, we study GFS structures of Au using TB potential of Mehl and Papaconstantopoulos (MP)[9] combined with a simulated annealing method[10]. We want to know how GFS energy is affected when atom relaxation is considered, and how the structure of the GFS changes due to the relaxation for the tight-binding potential. In the following, a general theory and method about the TB potential are presented firstly, then in the section 3, we give our calculated results and discussions about GSF, and finally, some conclusions are drawn out.

II. theory and method

In this work we use the tight-binding potential and combine a simulated annealing method to relax the generalized stacking fault structure of gold. The tight-binding potential originally is developed by Mehl and Papaconstantopoulos for transition and nobles metals[9]. This potential model stems from density functional theory(DFT)[11]. In the DFT theory, the total energy of a system of N atoms can be written as

$$E[n(\mathbf{r})] = \sum_i f(\mu - \epsilon_i)\epsilon_i + F[n(\mathbf{r})] \qquad (1)$$

where the first term is the band structure energy. In a self-consistent calculation the eigenvalues ϵ_i and charge density $n(\mathbf{r})$ are determined self-consistently via the Kohn-Sham equations[11], μ is the chemical potential, and the sum is over all electronic states of the system, $f(\mu - \epsilon_i)$ is the Fermi function. The functional $F[n(\mathbf{r})]$ contains the remaining part of the DFT total energy: the ion-ion interaction energy, the parts of the Hartree and Exchange-Correlations not included in the eigenvalue sums, and correction for double counting in the eigenvalue sums. In an earlier TB model the electronic band structure energy was determined from a parameterized Hamaltonian, while the remaining functional $F[n(\mathbf{r})]$ was parameterized by the

other means, such as, a pair potential method. In the TB model of Mehl and Papaconstantopoulos, they based on the fact that the DFT allows an arbitrary shift in the potential, and developed an alternative method of applying tight-binding to Eq. (1). By a shift[9] they transformed eq. (1) into the form of eq. (2):

$$E[n(\mathbf{r})] = \sum_i f(\mu' - \epsilon_i')\epsilon_i' \tag{2}$$

Thus, such a tight-binding method may solve the total energy problem of eq. (2), instead of eq. (1), and does not resort to an additional term.

Going a step further, Mehl and Papaconstantopoulos solved the problem by the two-center slater-Koster formulation[12] with a non-orthogonal basis. In this case, three types of parameters: on-site parameters, Hamiltonian parameters and overlap parameters need to be calculated. The on-site parameters represent the energy required to place an electron in a specific orbital and depends a local environment, Hamiltonian parameters represent the matrix elements for electrons hopping from one site to another, and overlap parameters describe the mixing between the non-orthogonal orbitals on neighbor sites. The eigenvalues ϵ' can be determined once these parameters are evaluated for a given structure. In the model, Mehl and Papaconstantopoulos gave on-site parameters, Hamiltonian parameters and overlap parameters the following analytical forms.

The on-site parameters vary with local environment and are defined as a Birch-like form

$$h_{i\alpha} = a_{\widetilde{i\alpha}} + b_{\widetilde{i\alpha}}\rho_i^{2/3} + c_{\widetilde{i\alpha}}\rho_i^{4/3} + d_{\widetilde{i\alpha}}\rho_i^2 \tag{3}$$

where $\widetilde{i}$ denotes the type of atom on site i, α expresses s, p, d orbitals, and the local environment ρ is determined by defining a pseudo-atomic density for each atom

$$\rho_i = \sum_{i\neq j} \exp[-\lambda_{\widetilde{ij}}^2 R_{ij}] F_c(R_{ij}) \tag{4}$$

In this expression λ is a parameter which depends on the atom types, R_{ij} is the distance between atoms i and j, F_c is an university cutoff function chosen to simplify the calculations.

$$F_c(R) = \{1 + \exp[(R - R_0)/l]\}^{-1} \tag{5}$$

The two-center Slater-Koster hopping terms (Hermiltonian parameters) are simply plonomials times the cut-off function.

$$P_\gamma(R) = (e_\gamma + f_\gamma R + \bar{f}_\gamma R^2)\exp[-g_\gamma^2 R] F_c(R) \tag{6}$$

where γ indicates the type of interaction (e.g. $ss\sigma$, $pd\pi$, etc.).

So does it, the overlap parameters are also assumed to have the same functional form as eq(6).

Finally, in this method, the potential parameters (λ, R_0, l, a, b, c, d, e, f, $\bar{f}$, and g,) are determined by requiring that the tight-binding method reproduce the first principles total energies and electronic band structures of fcc and bcc as a function of volume for these metals[9]. This method has been shown to give reliable structural behavior, elastic constants, phonon frequencies, vacancy formation energies, and surface energies for the fcc metals. In the present work, we use the method to study the stacking fault of gold. The potential parameters are the new set of potentials parameters for Au and may be obtained from the World Wide Web at http://cst-www.nrl.navy.mil/bind/. The Programs used in this work is from the static version 111 of Mehl. This program does not do calculations for atom relaxation. We have revised it and added a simulated annealing code to this program.

III. Generalized stacking fault structures and energies

As Mehl and Papaconstantopoulos did[9], we model the $< 112 >$ slip on a $(11\bar{1})$ slip plane of metal Au by constructing a supercell which consists of twenty close-packed $(11\bar{1})$ planes of Au atoms. One Au atom in each plane is part of the basis of the supercell. The primitive vectors of the supercell take the form

$$\begin{aligned} \mathbf{a}_1 &= \frac{1}{2}a_0\vec{y} + \frac{1}{2}a_0\vec{z} \\ \mathbf{a}_2 &= \frac{1}{2}a_0\vec{x} + \frac{1}{2}a_0\vec{z} \\ \mathbf{a}_3 &= (4 + \frac{q}{6})a_0\vec{x} + (4 + \frac{q}{6})a_0\vec{y} - (4 - \frac{q}{3})a_0\vec{z} \end{aligned} \tag{7}$$

where a_0 is lattice constant, q represents the stacking fault variable, and represents a displacement of the atom in the boundary plane along the fault vector $\vec{f}$ in the $< 112 >$ direction. When $q = 0$ the periodic crystal is a perfect fcc system $ABC|ABC$, where | denotes a "boundary plane". When $q = 1$, the atoms at the interface are in an hcp ordering, that is, the stacking at the interface is $ABC|BCA$ rather than $ABC|ABC$. In this calculation we only consider the relaxation of atom along the direction of $< 11\bar{1} >$. The atoms in the three atom layers that are the three nearest to and over the boundary plane and the atoms in the other three atom layers that are the other three nearest to and below it are allowed to relax. We define the first interlayer spacing as the spacing between two atom layers that are the nearest to the boundary plane, the second interlayer spacing as the spacing between the atom layer that is the first nearest to the boundary plane and the atom layer that is the second nearest to the boundary plane, and the third interlayer spacing as the spacing between the atom layer that is the second nearest to the boundary plane and the atom layer that is the third nearest to the boundary plane.

We set simplely the scheme for simulated annealing. First, we set an initial temperature to 50 K to run the program 1000 steps, and then the temperature drops to zero and the program is run for another 1000 steps.

As in all band structure total energy methods, the calculated total energy is determined by summing the eigen-

values over the first Brillouin zone of the lattice. We perform this calculation using a regular, uniformly space, and symmetrized k-point mesh, including the origin. The tight-binding methods is computational very efficient so to insure convergence we have used a large number of k points, 4808 in the irreduible part of the Brillouin zone of Eq. (7). This is equivalent to using a mesh of 1202 k points in the the irreducible Brillouinm zone of fcc lattice. The total energy is calculated by weighting the eigenvalues with a fermi distribution at a temperature of 5 mRy and then extrapolating to zero temperature. Our numerical results show in Fig. 1 and Fig.2., and the relaxed and unrelaxed SFE, anti-SFE, together with the results from experiments and first principles calculations are listed in Table 1.

Firstly, we see the unrelaxed and relaxed GSF curves for gold in Fig. 1. The horizontal axis denotes displacement variable q, and the vertical axis denotes energy per unit area in units of mJ m^{-2}. Either for relaxed one or for unlaxed one, the both curves have a skewed sinusoidal shape, as assumed by the early models of Frenkel[13], Mackenzie[14], and later, by Rice[15]. It is interesting to note that for the curves the unstability SFE (also calls it anti-SFE) reaches at a displacement $q/2$. This corresponds to one-half of the partial Burgers vector b_q. This is a value which one would expect from geometrical considerations. The first principles calculations and embedded-atom potentials also find such shape of GSF for Cu, Al, and Ni[5]. This is in agreement with the present TB potential calculations. From the figure we also note that there is a far more obvious relaxation at the site of the unstability SFE ($q = 1/2$) than the site of SFE ($q = 1$). As well know, the formation of a stacking fault depends on not only SFE but also anti-SFE. The larger the anti-SFE is, the more difficult to form a stacking fault is. Thus, in order to obtain an accuracy anti-SFE, it is necessary to include an atom-scale relaxation. We list relaxed SFE (γ_{sf}), anti-SFE (γ_{us}) for Au, together with the results from the first principles calculations, as well as, experiments in table 1. The experimentally determined value of γ_{sf} of Au is at the range of 10-60 mJ m^{-2}[8]. In the experiment, the precise determination of SFE is some difficult and it depends on experimental technique and has errors of unknown magnitude. By forming weighted mean value, the SFE of Au is 50 mJ m^{-2}[8]. The results from the first principles calculations is 50 mJ m^{-2} or so[6], [7]. In our calculations the SFE is 46 mJ m^{-2}. Thus, the result using the TB potentials of MP is in extreme agreement with the first principles calculations and the experiments. In the calculations of MP, the unrelaxed SFE and anti-SFE are 50 and 129 mJ m^{-2} for Au. In our calculations the values are 50 and 127 mJ m^{-2}, respectively, and in good agreement with their calculations. From the table and Fig. 1 we also see that the SFE is reduced by 6% and the anti-SFE is reduced over 20% by atom relaxation.

Now let us see the atom-scale structure about generalized stacking fault. Fig. 2 shows the changes of atom layer spacings by the atom-scale relaxation. From the figure we can see that the first interlayer spacing have the largest change and contracts within the whole range of q considered while the third interlayer spacing expands. The second interlayer expands firstly and then contracts. At the site of anti-SFE ($q = 1/2$) there is the largest relaxation. In addition, we find that the first interlayer spacing has far larger relaxation than the other two interlayer spacings. Perhaps, these results are a possible clue that in the gold the interface does not trend to cleave because in this simulation the atoms in the interfaces trend inter-joint. In the site of SF ($q = 1$) the interface structure is a hcp-like, we calculate its c/a. We obtain that this value is 1.628. It is close to the ideal value 1.633 very much although it is tiny smaller than the ideal value. These results are also some interesting to further test the accuracy of the potential model when a more accuracy calculation, such as, the first principles calculations, is performed.

IV. Conclusions

We use TB potential of MP to study the generalized stacking fault. The potential predicts the properties of generalized fault very well. Firstly, the stacking fault energy is calculated to be equal to 46 mJ m^{-2} and in very good agreement with the experiment value (50 mJ $m^{-}2$) and the first principles calculations (45 mJ m^{-2}, 59 mJ m^{-2}). The skewed sinusoidal shape of the generalized stacking energy with the displacement variable q is identical to the theoretical predictions of Frenckle, Mackle and Rice. The site of anti-SFE is also predicted to be the same as the ideal value (1/2 of the partial Burgers Vector) from geometrical considerations. Also, the potential predicts that the first interlayer spacing contracts for the all q considered while the third interlayer spacing expands. The second interlayer spacing firstly expands and then contracts with the variation of q from 0 to 1. The first interlayer spacing has far larger relaxation than the other two interlayer spacings. Perhaps, these are a possible clue that in the gold the interface does not trend to cleave because in this simulation the atoms in the interfaces trend inter-joint. In the calculations we find that there are the largest relaxation in the site of anti-SFE. Finally, the potential predicts that the c/a of the stacking fault structure is slightly smaller than the ideal value: 1.633. In addition, the results about relaxed GSF structures may be also used to further test the accuracy of the potential model when a more accuracy calculation is available.

Acknowledgments

The authors thank Prof. Michael J. Mehl at Naval Research Laboratory, Washington, for his providing the TB program of static version 111. This work is supported by a Singapore-MIT Alliance Research Grant.

References

[1] M. J. Mehl, D. A. Papaconstantopoulos, N. Kioussis and M. Herbranson, Phys. Rev. B **61**, 4891(2000)

[2] D. L. Medlin, S. M. Foiles, and D. Cohen, Acta mater. **49**, 3689(2001)

[3] J. Cai, D. S. Wang, S. J. Liu, S. Q. Duan, and B. K. Ma, Phys. rev. B **60**, 15691(1999)

[4] M. A. Merers, O. Vohringer and V. A. Lubarda, Acta mater, **49**, 4025(2001)
[5] J. A. Zimmerman, H. Gao and F. F. Abreham, Modeling Simul. Mater. Sci. Eng. **8**, 103(2000)
[6] N. M. Rosengaard and H. K. Skriver, Phys. Rev. B **47**, 12865(1993)
[7] S. Schweizer, C. Elsasser, K. Hummler, and M. Fahnle, Phys. Rev. B **46**, 14270(1992)
[8] P. C. J. Gallagher, Metall. Trans. **1**, 2429(1970)
[9] M. J. Mehl and D. A. Papaconstantopoulos, Phys. Rev. B **54**, 4519(1996)
[10] W. H. Press, S. A. Teubolsky, W. T. Vetterting, and B. P. Flannery, Numerical recipes in Fortran 77: The Art of Scientific Computing 2ed Vol 1 of Fortran Numerical Recipes, (Cambridge University Press, 1997), p443.
[11] P. Hohenberg and W. Kohn, Phys. Rev. **136**, B864(1964); W. Kohn and L. J. Sham, Phys. Rev. **140** A1133(1965)
[12] J. C. Slater and G. F. Koster, Phys. Rev. **94**, 1498(1954)
[13] J. Frenkel Zur theorie de elastizitatsgrenze und der festigkeit Kristallinischer Korper Z. Phys. 37, 572(1926)
[14] Mackenzie J. K. PhD Thesis Bristol University, 1949
[15] J. R. Rice, Dislocation nucleation from a crack tip: an analysis based on the Peierls concept, J. Mech. Phys. solids **40**, 239(1992)

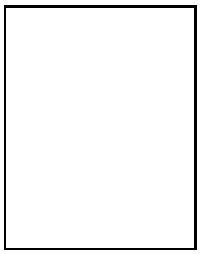

Jun Cai and Jian-Sheng Wang The Singapore-MIT Alliance, E4-04-10, 4 Engineering Drive 3, Singapore 117576 and Department of Computational Science, National University of Singapore, 2 Science Drive 2, Singapore 117543

Table 1: Stacking fault energy (SFE) and anti-SFE for Au. The two rows of data are given, the first one is for unrelaxed ones, the second one for the relaxed.

Energy (mJ m^{-2})	This work	Exp.	the first principles	MP
$anti-SFE$	127			129[a]
	102			
SFE	50		59[b],45[c]	50[a]
	46	50[d]		

[a] Ref. [1]
[b] Ref. [6]
[c] Ref. [7]
[d] Ref. [8]

Figure captions:

Fig. 1. Generalized stacking fault energy as a function of parameter q in Eq. (7) for metal Au. The circle line for the calculations without relaxation and the square line for the calculations with relaxation.

Fig. 2. The changes of interlayer spacings (in the unit of au%) as a function of parameter q in Eq. (7) for metal Au. The circle line for the change of the first interlayer spacing, the square line for the change of the second interlayer spacing, and the diamond line for the change of the third interlayer spacing. Negative values are contractions in interlayer spacings.

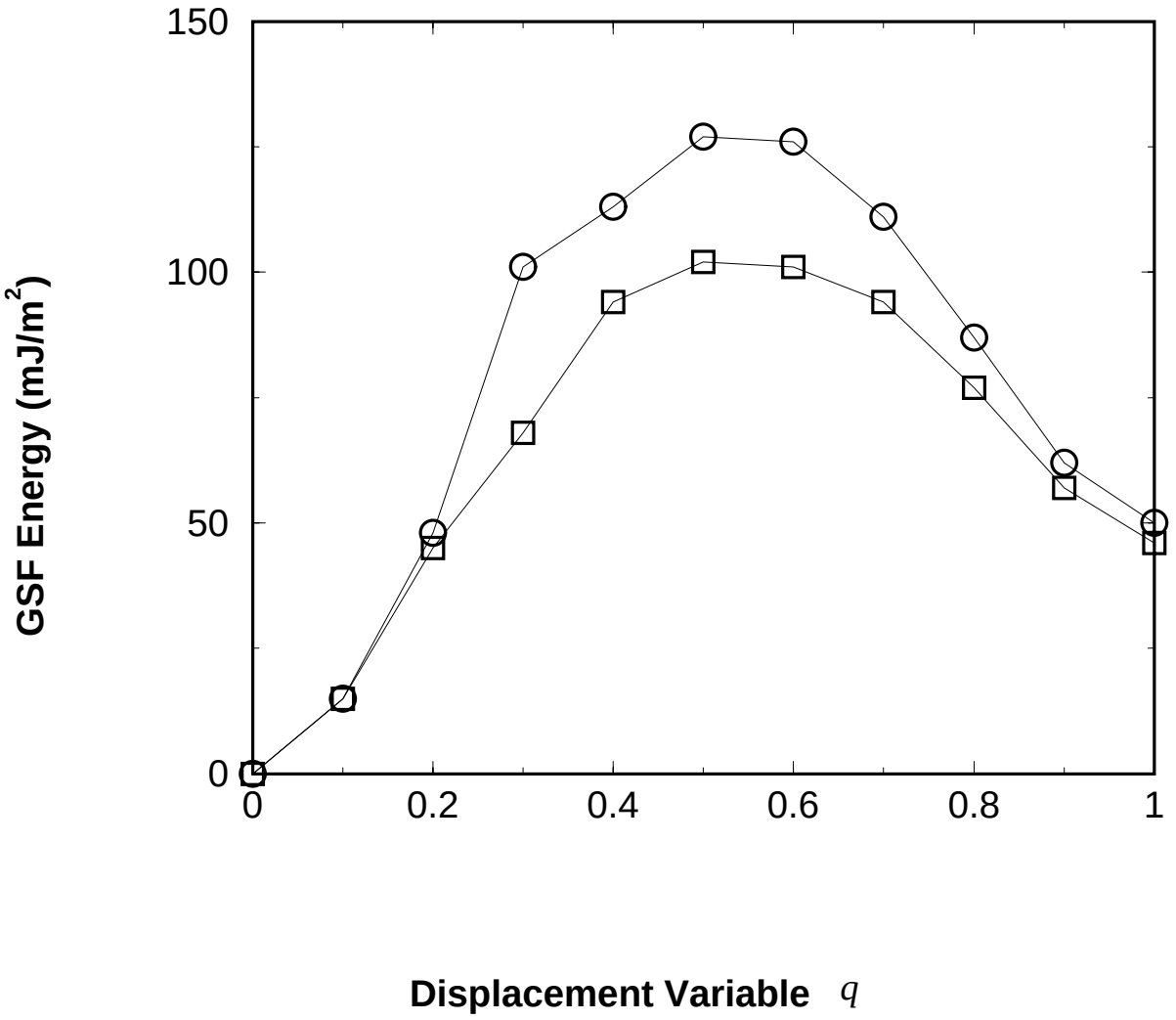

Fig. 1. J. Cai and J.−S. Wang

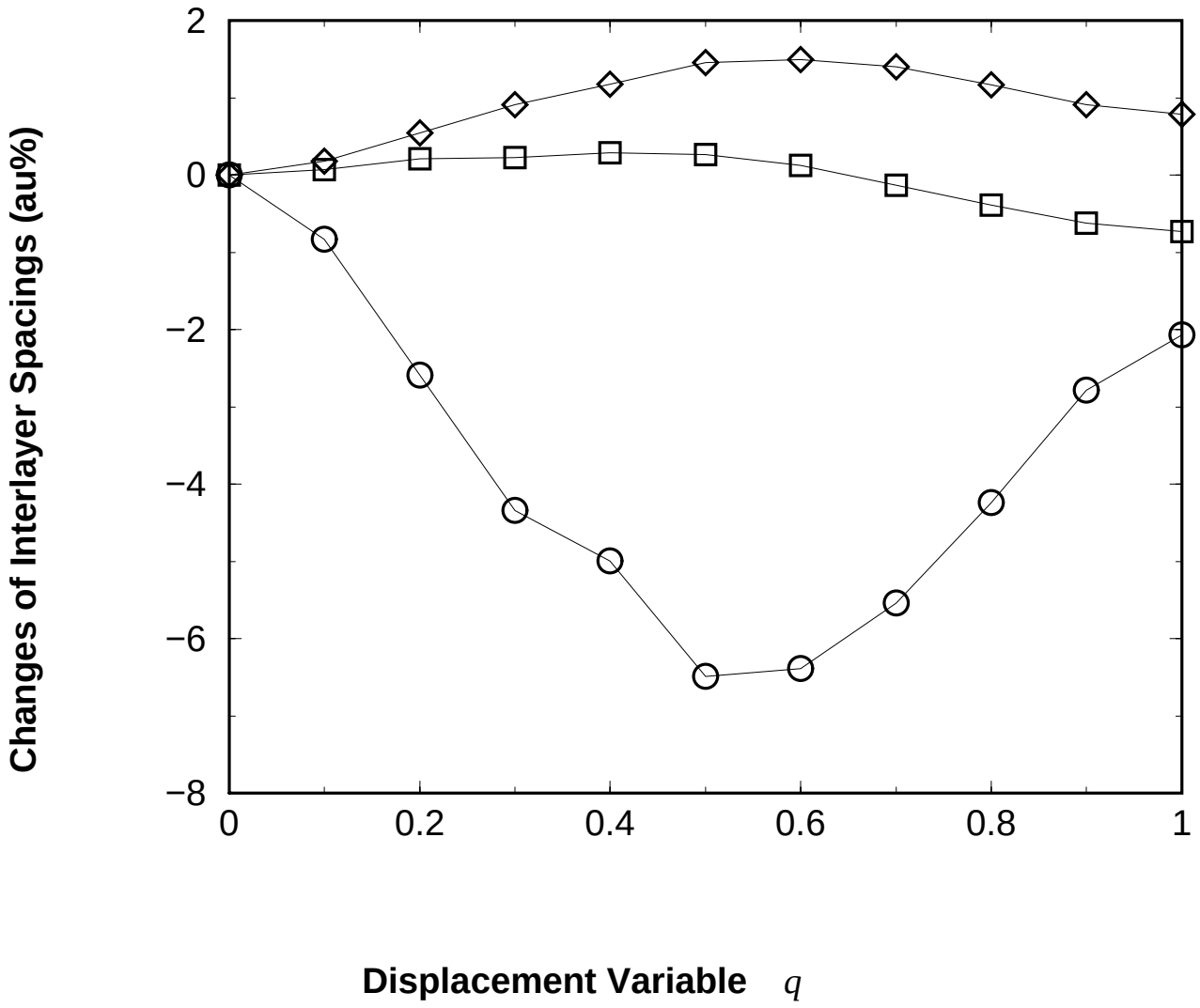

Fig. 2. J. Cai and J.−S. Wang